

# Examining Chaotic Behaviour in a Non-Linear Chaotic Circuit

Kabir Dhillon<sup>\*</sup> and Malcolm Pidsosny<sup>†</sup>

*Dept. of Physics, Simon Fraser University, Burnaby, BC, Canada*

(Dated: March 31, 2023)

## Abstract

We create a non-linear chaotic circuit to examine methods used to analyze chaotic behaviour. The three methods we examine are bifurcation plots, phase portraits and return maps. Each method provides a unique insight into the system and can be used to determine the presence of chaos, stability of fixed-points, and the number of periods present in the system. The experimental results show that each method is effective in analyzing chaotic systems, providing insights into the behavior of the system.

---

<sup>\*</sup> [ksd12@sfu.ca](mailto:ksd12@sfu.ca)

<sup>†</sup> [mgp3@sfu.ca](mailto:mgp3@sfu.ca)

Chaotic systems are found in many natural scenarios, however these scenarios are notoriously challenging to analyze. A classic example of this is a double pendulum which is a complexity added to a simple system to create chaos. Even the simpler version results in chaos, where a single pendulum at large amplitudes results in chaos. Many very common scenarios are similar to this, where changes in initial conditions will cause the system to become chaotic. Therefore developing analytical methods becomes vital to gaining insight into a chaotic system. In this experiment, we create a non-linear chaotic circuit to demonstrate three different methods of analyzing chaotic behaviour. The three methods used are bifurcation plots, phase portraits, and return maps. Each of these methods provides unique insights into the system and can be used to determine the presence of chaos, stability of fixed-points, and the number of periods present in the system. The aim of this experiment is to showcase the effectiveness of these methods in analyzing chaotic systems specifically a non-linear chaotic circuit.

In this experiment we use a non-linear electronic circuit to study chaotic behaviour. The non-linear circuit used can be modelled by the third order differential equation [2],

$$\ddot{x} = -A\ddot{x} - \dot{x} + D(x) - \alpha. \quad (1)$$

A system described by this equation results in chaos and is non-linear due to the non-linear element  $D(x)$  which is proportional to  $-\min(x, 0)$  [2]. The  $\alpha$  term represents a system parameter that only changes when the system itself changes. The behaviour of the system can be changed by varying the control parameter  $A$ . At large values of  $A$ , the system has fewer periods of oscillation making the system easy to analyze. As  $A$  is decreased the system undergoes bifurcations where the period of oscillations increase at each bifurcation point [1]. Eventually, the system has many periods of oscillations and becomes very sensitive to initial conditions which is where the system is considered to have entered a chaotic region [1]. The chaotic region can be analyzed using a bifurcation plot which plots the number of periods at each value of  $A$  [1]. The plot shows which values of  $A$  are bifurcation points. By examining the bifurcation plot, we can determine which values of  $A$  lead to a non-chaotic system with a low number of periods and which produce a chaotic system with a high number of periods.

Another way to identify chaos within a system is by creating a phase portrait. A phase portrait can be described using the equation [1],

$$\dot{x} = f(x). \quad (2)$$

An analytical solution to this equation is extremely difficult to determine and more insight is gained from the qualitative aspects of the plot [1]. A closed orbit within a phase portrait represents a periodic solution to the system [1]. In non-chaotic region, the phase portrait would display simple smooth curves, while in chaotic regions the curves would be open and irregular [1]. The chaotic regions would also display many more curves as those regions contain more periods than the non-chaotic regions.

A chaotic region can be further analyzed using a return map. A return map plots  $x_n$  against the value of  $x_{n+r}$ . The qualitative aspects of the return map plot show useful aspects of chaotic regions. A fractal pattern within a return map shows the region is a chaotic region [2]. A fractal can be characterized by a splitting of a curve or a cluster of points at a certain area of a curve. Furthermore, periodic orbits can be observed within chaotic regions however these are unstable [1]. The stability can be determined by examining fixed-points which fall along the  $y = x$  line. A fixed-point is stable if  $|f'(x)| < 1$  at that point, and unstable if  $|f'(x)| > 1$  [1].

The circuit created in this experiment uses integrating sub-circuits. An integrating circuit converts the input voltage into its integrated form (e.g., turns a square wave into a triangle wave)[3]. Typically, a capacitor is enough to create an integrating circuit. However, op-amps are often used in integrating circuits because they can buffer the output voltage to be roughly the same as the input voltage[3]. This buffering prevents significant voltage drop throughout the entire circuit, making the results at each node easier to analyze. An op-amp is able to do this due to the op-amp golden rules which are [3]:

- The input current is practically 0.
- The output makes the voltage difference between the two inputs 0.

A capacitor would typically have a voltage drop due to the discharge however the op-amp will counteract this resulting in a voltage output similar to the input.

The circuit (shown in fig.1a) describes the system created in this experiment [2]. Applying Kirchoff's rules and the golden rules for an op-amp at each node results in the equation [2],

$$\ddot{x} = -\frac{R}{R_v}\ddot{x} - \dot{x} + D(x) - \frac{R}{R_0}V_0. \quad (3)$$

Showing that in this setup, the value of  $A$  is  $\frac{R}{R_v}$  and the control parameter can be varied using the value of  $R_v$ . The value of  $R_v$  in this system was varied in  $1k\Omega$  increments from  $50k\Omega$  to

130k $\Omega$ . The  $\alpha$  system parameter is then  $\frac{R}{R_0} V_0$  and is proportional to the initial voltage  $V_0$ . The resistor without any label within the circuit are all  $R = 47k\Omega$  and the capacitors with no labels are all  $C = 1nF$ . The value of  $R_0$  is 148k $\Omega$  and the input voltage is  $V_0 = 0.5V$ . The input voltage is from a function generator set to a DC input at  $0.25V_{pp}$  however due to the high output impedance, the voltage becomes approximately double. Applying the same rules along the nodes of fig.1b and using Shockley's equation at the diodes gives an equation for the non-linear element  $D(x)$  which can be approximated as [2],

$$D(x) = -\frac{R_2}{R_1} \min(x, 0). \quad (4)$$

The op-amps used in fig.1 are the LF411 and the diodes used in fig.1b are the IN4001. The value of the resistors in fig.1b are  $R_1 = 0.99k\Omega$  and  $R_2 = 5.59k\Omega$ .

The theoretical bifurcation plot fig.2b was created by numerically integrating the ODE in Eq.3 with the initial values of the setup creating voltage-time plots. The bifurcation plot of the data in fig.2a was created by measuring the voltage at the node  $x$  at each value of  $R_v$ . To determine the number of periods at each  $R_v$ , the number of unique peak amplitudes in each voltage-time plot was found. The peak voltages at the node  $x$  is then plotted for each  $R_v$  showing the number of periods at each  $R_v$ . However, initially the result did not resemble a bifurcation plot and required the noise to be removed since peaks that would be the same were slightly shifted down or up due to noise. The noise in the data was mostly removed by using a fast fourier transform on the voltage time-data [2]. The frequencies that were very low and high associated with noise were removed and the fourier transform was inverted. The result was a much cleaner voltage-time plot.

The phase portrait was created by numerically differentiating the voltage at the node  $x$  to get the value of  $\dot{x}$ . The numerical derivative was found by using a Savitsky Golay filter setting the polynomial order to 5 and the step size set to a value of 0.1. The data used was the voltage-time plots with the noise removed using the FFT. A phase portrait was made at each  $R_v$  value, however fig.3 only show ones that represent unique regions in the data. An equivalent way of finding  $\dot{x}$  would be to measure the voltage at the node  $V_1$  on fig.1 since it has a voltage equivalent to  $-\dot{x}$  [2]. The first and second return maps were created by plotting the voltage at the node  $x$  along the x-axis and the voltage measurement following it on the y-axis. The theoretical return maps were created using the exact same steps however, the data used was from the theoretical voltage-time plots.

Fig.2a shows the bifurcation plot of the data collected. The general shape of the plot resembles the theoretical which can be easily seen in fig.2c. From the experimental plot, we can see the initial bifurcation point is at  $R_v \approx 53k\Omega$ . Furthermore, the chaotic region can be identified as being between an  $R_v \approx 70k\Omega$  and  $R_v \approx 100k\Omega$  which can be seen from the number of periods at each  $R_v$  [1]. The initial bifurcation from the theoretical plot in fig.2b occurs at the same point however, the chaotic region is between an  $R_v \approx 70k\Omega$  and  $R_v \approx 105k\Omega$ . Also on the theoretical plot, the number of periods decreases and there is a "hole" within the chaotic region between an  $R_v \approx 80k\Omega$  to  $R_v \approx 83k\Omega$ . This "hole" also occurs in the experimental bifurcation plot but, it occurs between  $R_v \approx 78k\Omega$  to  $R_v \approx 79k\Omega$ . Looking at the superimposed plots in fig.2c, the experimental data has a larger voltage range which is most likely due to the noise in the data. Also, looking at the endpoints in Fig.2a between  $R_v \approx 110k\Omega$  to  $R_v \approx 130k\Omega$  and comparing it to Fig.2b shows there is still noise within the data that impacted some of amplitudes plotted.

Fig.3 shows the phase portraits at different values of  $R_v$ . The values of  $R_v$  were chosen to show phase portraits in different regions. Fig.3a shows the phase portrait at an  $R_v$  value of  $50k\Omega$ . The region showcased is a non-chaotic region with a one period solution (as seen in fig.2a). The curve is a closed-orbit and is smooth with only one curve showing this region is non-chaotic with a one-period solution [1]. Fig.3b and fig.3c shows the phase portrait at an  $R_v$  value of  $73k\Omega$  and an  $R_v$  value of  $95k\Omega$  respectively. The curves are smooth and closed, but there are many of them showing many periods and the shapes are irregular. Therefore, the regions can be considered chaotic and looking at this region in fig.2a we see this is a chaotic region [1]. Fig.3d shows the phase portrait at an  $R_v$  value of  $128k\Omega$ . There are two smooth curves that are closed showing this is a non-chaotic region with a two period solution. Again, looking at the bifurcation plot we see that this region is non-chaotic and has 2 periods [1]. The scale of the y-axis is very large since the step size for the numerical derivative was very small. In general, the scale does not change the results too much as the qualitative aspects of the plot are used to analyze chaos rather than the quantitative results. In fig.3b and fig.3c, there is one line that connects to a curve but is discontinuous at one side. The cause of this is when the data collection was ended, the line is most likely another curve being generated but the data stops there.

Fig.4 shows the first and second return map at an  $R_v$  of  $73k\Omega$ . The green points are the experimental data and the black points are the theoretical. The cluster of points near the

$y = x$  line in fig.4a show there is a fractal pattern at that point, which means there is chaos at this  $R_v$  value [2]. The shape of the curve shows that the function applied to  $x$  in eq.2 is most likely a 2nd-order polynomial. Observing the intersection at the  $y = x$  line, we see that  $|f'(x)| > 1$  at that fixed point showing it is unstable [1]. Therefore, there is an unstable period-one orbit in this chaotic region. Fig.4b shows the second return map. There is again a cluster of points near the  $y = x$  line showing there is a fractal pattern, which again shows there is chaos at this  $R_v$  value [2]. The shape of this curve is different from the first return map and shows that the function applied to  $x$  in eq.2 is most likely a 3rd-order polynomial. Observing the intersection at the  $y = x$  line, we see that  $|f'(x)| > 1$  at that fixed point showing it is unstable [1]. Therefore, there is an unstable period-two orbit in the chaotic region. The period-one orbit can be seen in the time series in fig.5. Between the -0.004s and -0.002s there is only one period present however, this only continues within that time period showing the instability of this period-one orbit.

All three methods can be used to determine if a region is chaotic. However, they each provide a unique analysis of the region. A bifurcation plot gives an overview of the system and can be used to determine the approximate areas where chaos occurs. Also it can be used to determine the number of periods present at specific values of  $A$ . A phase portrait can be used to visually investigate specific values of  $A$  and how it evolves over time. The return map can be used to determine the stability of fixed-points and determine periodic orbits in chaotic regions. The qualitative aspects of each method are easier to determine with data with less noise which can be reduced using a fast fourier transform. Overall, using all three methods can provide insight chaotic systems that typically challenging to analyze.

- 
- [1] S. H. Strogatz, *Nonlinear Dynamics and Chaos*, 2nd Ed., 2015, reprinted by CRC Press, 2018
  - [2] K. Kiers, D. Schmidt and J. C. Sprott, "Precision measurements of a simple chaotic circuit", *Am. J. Phys.* **72**, 503–509 (2004).
  - [3] P. Horowitz and W. Hill, *The Art of Electronics*, Cambridge University Press

## FIGURES

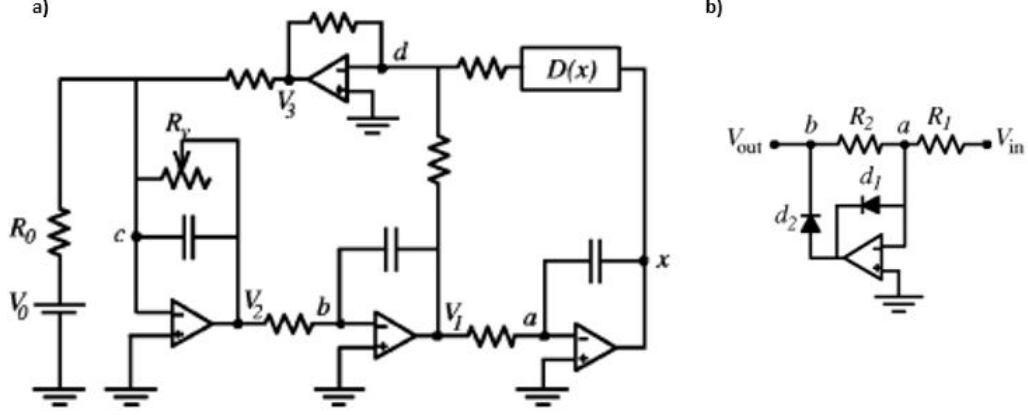


FIG. 1. a) is the circuit diagram [2] described by the Eq.3. The values for the resistors are  $R_0 = 148k\Omega$  while the  $R_v$  varies from  $50k\Omega$  to  $130k\Omega$ . The resistors with no label are all  $R = 47k\Omega$  and the capacitors with no label are all  $C = 1nF$ . The  $V_0$  is the initial input voltage and is  $V_0 = 0.5V$ . The labels  $V_1$ ,  $V_2$  and  $x$  all represent nodes where  $V_1 = -\dot{x}$  and  $V_2 = \ddot{x}$ . All the op-amps used are the LF411. b) is the circuit diagram of the non-linear element  $D(x)$  from a). The resistor values in  $D(x)$  are  $R_1 = 0.99k\Omega$  and  $R_2 = 5.59k\Omega$ . These resistor values were chosen since this results in  $\frac{R_2}{R_1} \approx 6$  [2]. The diodes used are IN4001. The voltage input at the node  $V_{in}$  is from  $x$  so Eq.4 can be used to describe the output voltage at  $V_{out}$ .

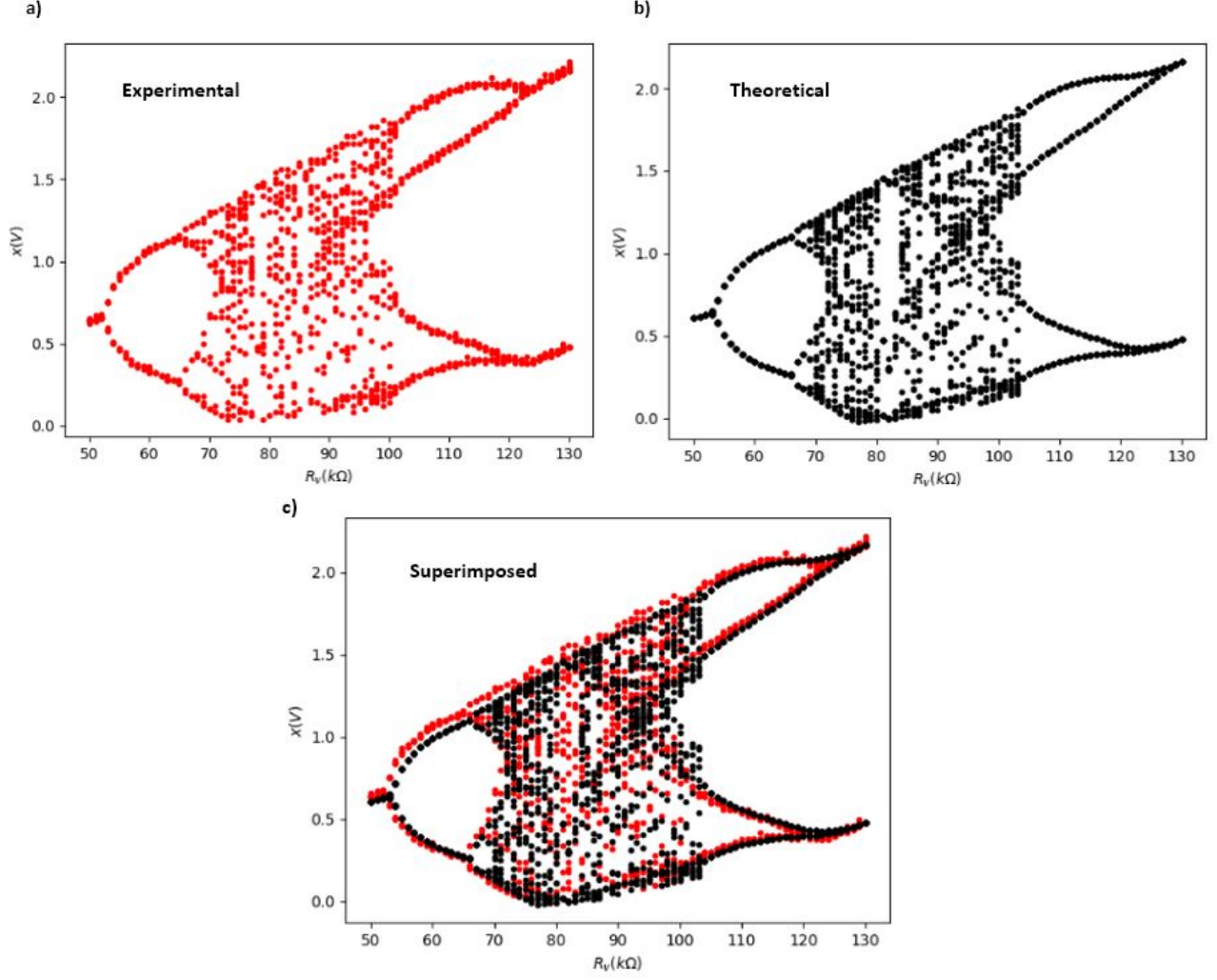


FIG. 2. The bifurcation plots of the experimental (a), theoretical (b) of the circuit in fig.1 along with the superimposed plot (c) of the theoretical and experimental. The plots all have  $R_v$  in  $k\Omega$  along the x-axis and the voltage peaks at the node x along the y-axis. The experimental data was found by finding the all the peak voltages from the collected voltage-time plots at the varying  $R_v$  values. The theoretical data was determined by simulating a voltage-time plot at each  $R_v$  value using Eq.3 and finding the peak voltages. The solutions to Eq.3 needed to find peak voltages was found by numerically integrating the ODE with the initial values from our setup.



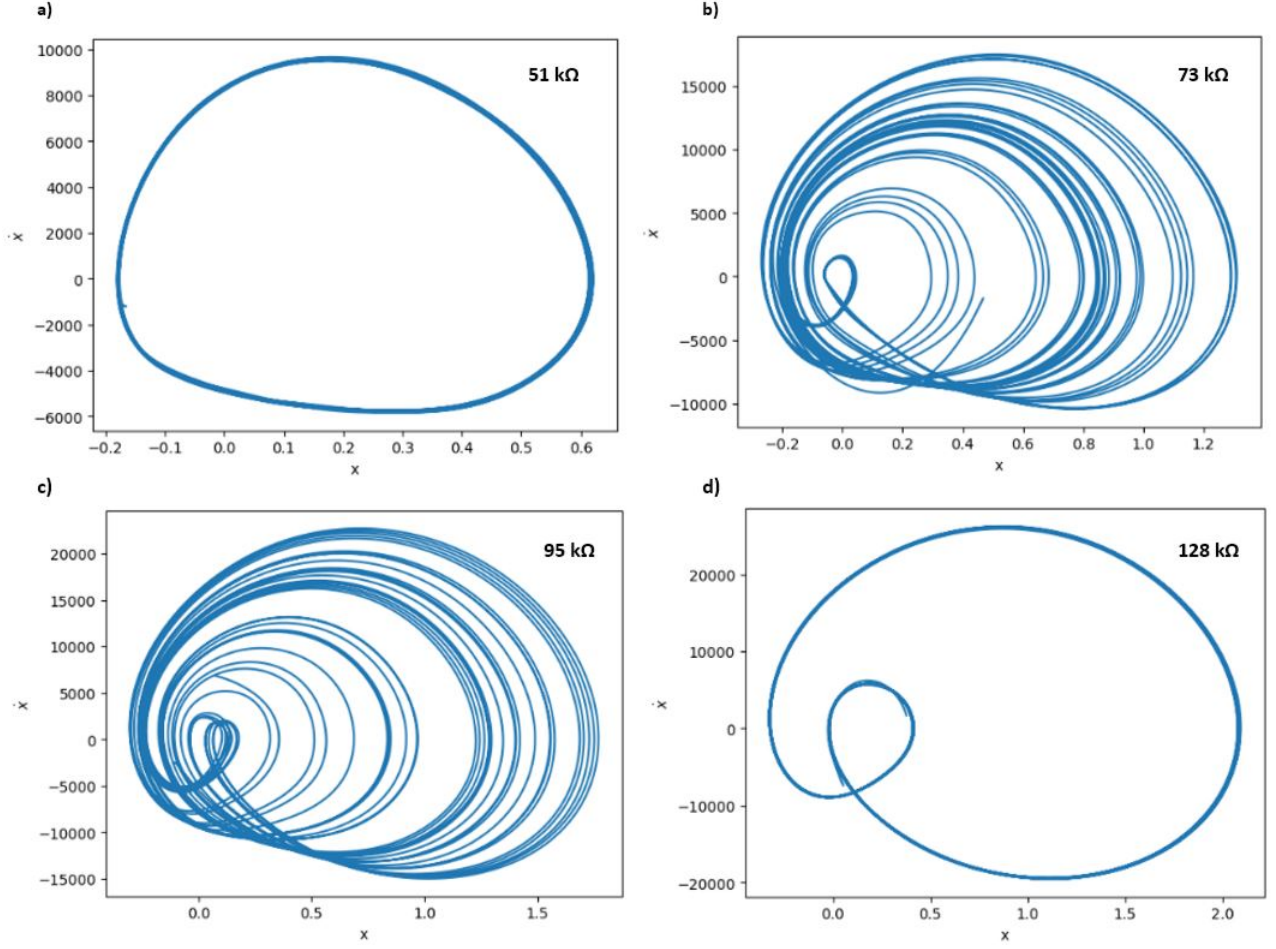


FIG. 3. Phase portraits found from the experimental voltage time plot and Eq.2. The value of  $x$  is along the x-axis and  $\dot{x}$  along the y-axis. The  $\dot{x}$  was found by taking the numerical derivative of  $x$  using a Savitzky-Golay filter. Before this, the data was also "cleaned" by taking the fourier transform of the voltage-time plot and getting rid of low and high frequency values effectively getting rid of most of the noise. The y-axis scale is extremely large since the step size used in the numerical derivative was very small (0.1). a) represents the phase portrait at  $R_v = 51 \text{ k}\Omega$ , b) represents the phase portrait at  $R_v = 73 \text{ k}\Omega$ , c) represents the phase portrait at  $R_v = 95 \text{ k}\Omega$ , and d) represents the phase portrait at  $R_v = 128 \text{ k}\Omega$

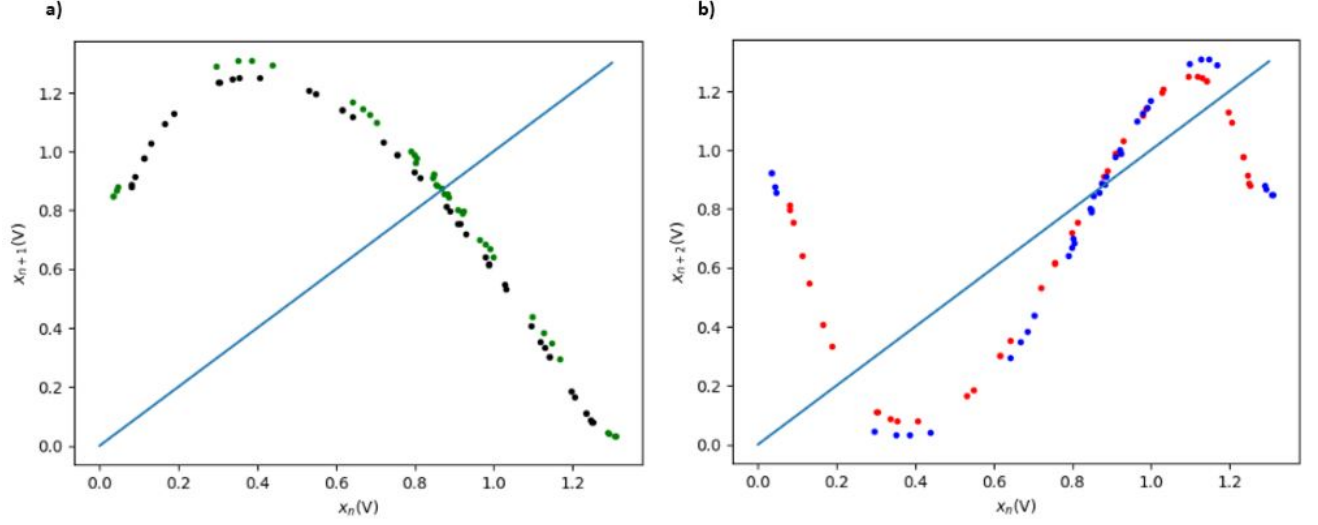


FIG. 4. a) shows the first return map at  $R_v = 73k\Omega$ . The  $x_n$  value is along the x-axis and the  $x_{n+1}$  along the y-axis. The green is the experimental and the black is the theoretical. The  $y = x$  line is there to examine the intersection point between it and the data to determine an unstable orbit. b) shows the second return map at  $R_v = 73k\Omega$ . The x-axis is the same as a), but the y-axis is now  $x_{n+2}$ . The red represents the theoretical while the blue is experimental. The experimental data for both a) and b) was also "cleaned" by taking the fourier transform of the voltage-time plot and getting rid of low and high frequency values to clear noise.

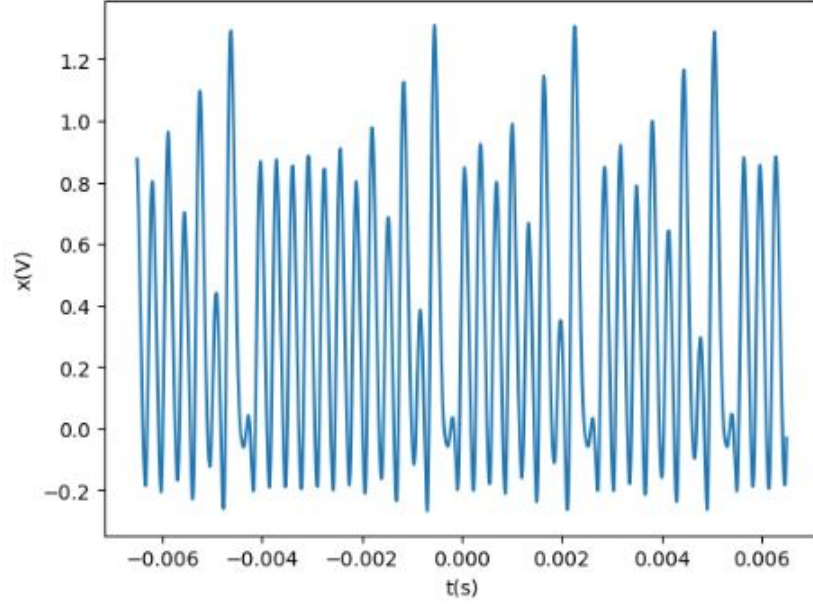


FIG. 5. Voltage-time plot at  $R_v = 73k\Omega$ . The data was fourier transformed to get rid of high and low frequencies to reduce noise. The plot shows only a section of the entire voltage-time plot at  $R_v = 73k\Omega$  where the one period and two period cycle within a chaotic region can be shown.